Requirements for Setting-Less Protection Schemes

A. P. Sakis Meliopoulos, *Fellow*, *IEEE*, George J. Cokkinides, *Senior Member*, *IEEE*, Sungyun Choi, *Student Member*, *IEEE*, Yonghee Lee, *Student Member*, *IEEE*,

***Abstract*--The numerical relay increased its domination to the point that today has almost completely displaced electromechanical and solid state relays. The numerical relays today, by and large, they simply mimic the logics that are developed for the electromechanical relays but with much more flexibility. Because numerical relays can pack many protection functions in one device, numerical relays are multifunctional. The increased functionality has resulted in more complex protection schemes with complex settings that many times lead to inconsistencies and possibility of improper protection actions.**

A new protection scheme is proposed that does not require settings. The approach is based on dynamic state estimation. Specifically, the proposed protection scheme is based on continuously monitoring terminal voltages and currents of the component and other possible quantities such as tap setting, temperature, etc. as appropriate for the component under protection. The monitored data are utilized in a dynamic state estimation that continuously provides the dynamic state of the component. The dynamic state is then used to determine the health of the component. Tripping or no tripping is decided on the basis of the health of the component.

The paper presents the approach, the dynamic state estimation and the definition of component health. The computational procedure is also outlined. Numerical experiments are presented to validate the method. Finally an evaluation of feasibility is provided based on present day microprocessor capabilities and it is concluded that present day microprocessors do have the computational power required by the proposed approach.

***Index Terms*--Nonlinear dynamic systems, dynamic state estimation, external and internal faults, component protection.**

I. Introduction

The numerical relay with present day high performance microprocessor has replaced the electromechanical and solid state relays. Such numerical relay can perform multiple protection functions. The multifunctional capability can cause complex coordination problems. The complexity can cause inconsistencies and the incorrect operation of relay, thus degrading security or dependability. These limitations of numerical relays are mainly due to the fact that the traditional numerical relay are monitoring a specific quantity or quantities (e.g., currents and/or voltages) and trip circuit breakers when a quantity or quantities enter a certain area. However, it is possible that the specific quantity or quantities do not always indicates the health of the component under protection, i.e. the condition may be a tolerable condition for which tripping is not warranted. There are other examples that present relaying approaches may not properly detect an intolerable condition. An example is shown in Figure 1. A fault near the neutral of a three-phase transformer may not be detected with the usual settings of transformer protection schemes.

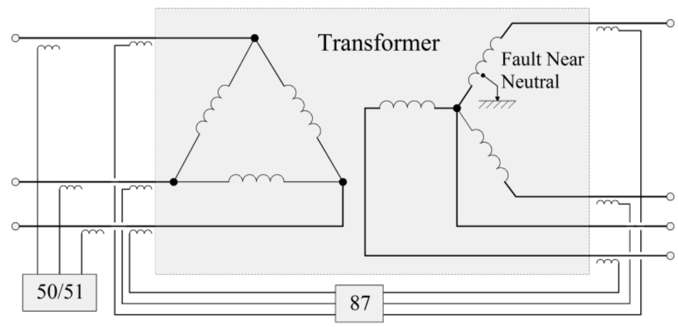

Figure 1. Transformer Overcurrent and Differential Protection

For a fault near the neutral, the overcurrent or the differential protection of the transformer will not detect this fault with usual transformer protection settings.

Another known protection issue is the fault induced delayed voltage recovery. Successfully cleared faults in transmission systems create overcurrent in distribution systems owing to the fault-induced delayed voltage recovery (FIDVR) phenomenon described in Figure 2. Specifically, during the fault the voltages are depressed causing the slowdown of rotating electrical machinery. When the fault is cleared the rotating machinery tries to accelerate to full speed, drawing very high currents and creating voltage drops that delay the recovery of the voltage. During this period the currents in distribution feeders may be high and they may cause the false tripping in this case of the feeder breakers.

False relay operations have been the major challenge in transformer protection, and thus many protection algorithms [1-3] that increase security have been developed: time-delay settings in the differential relays, the desensitization of relays during an inrush condition, the consideration of voltage, the harmonic restraint method, waveform shape identification, and the dwell time method. Nevertheless, these algorithms are inefficient in that they sometimes fail to identify the transformer inrush because of improper relay settings. Moreover, the algorithms can compromise dependability or speed according to their relay settings.

A. P. S. Meliopoulos, G. J. Cokkinides, S. Choi, and Y. Lee are with the School of Electrical and Computer Engineering, Georgia Institute of Technology, Atlanta, GA 30332-0250, USA (e-mails: sakis.m@gatech.edu, cokkinides@comcast.net, sungyun.choi@ieee.org, and yongalee@gatech.edu)

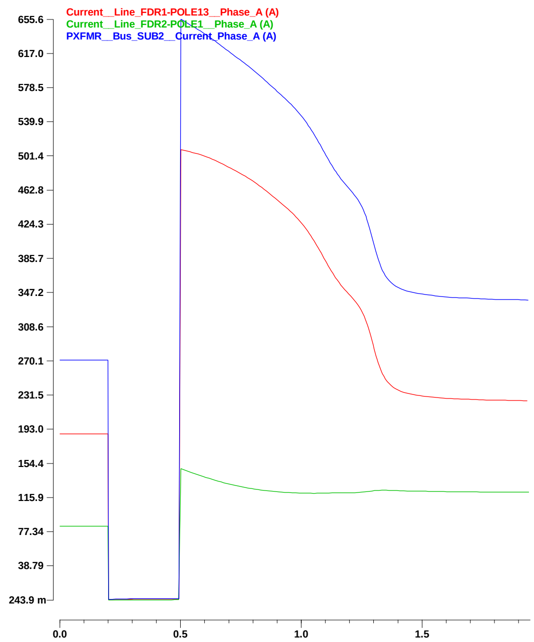

Figure 2. Feeder Overcurrent During Fault-induced Delayed Voltage Recovery

We present a new approach towards protection schemes that they do not need settings and coordination with other relays.

II. PROPOSED COMPONENT PROTECTION METHOD

For more secure protection of power components such as transmission lines, transformers, capacitor banks, motors, generators, etc., this paper proposes a method that continuously monitor the dynamic model of the component under protection via dynamic state estimation. Specifically, the proposed method extracts the dynamic model of the component under protection via dynamic state estimation [10-13]. The dynamic model of the component accurately reflects the condition of the component and the decision to trip or not to trip the component is based on the condition of the component irrespectively of the parameter of condition of other system components. Figure 3 illustrates this concept. The proposed method requires a monitoring system of the component under protection that continuously measures terminal data (such as the terminal voltage magnitude and angle, the frequency, and the rate of frequency change) and component status data (such as the tap setting and the temperature). The dynamic state estimation processes these measurement data and extracts the real time dynamic model of the component and its operating conditions.

After estimating the operating conditions, the well-known chi-square test calculates the probability that the measurement data are consistent with the component model (see Figure 4). In other words, this probability, which indicates the confidence level of the goodness of fit of the transformer model to the measurements, can be used to assess the health of the transformer. The high confidence level indicates a good fit between the measurements and the model, which indicates that the operating condition of the component is normal. However, if the component has internal faults, the confidence level would be almost zero (i.e., the very poor fit between the measurement and the transformer model).

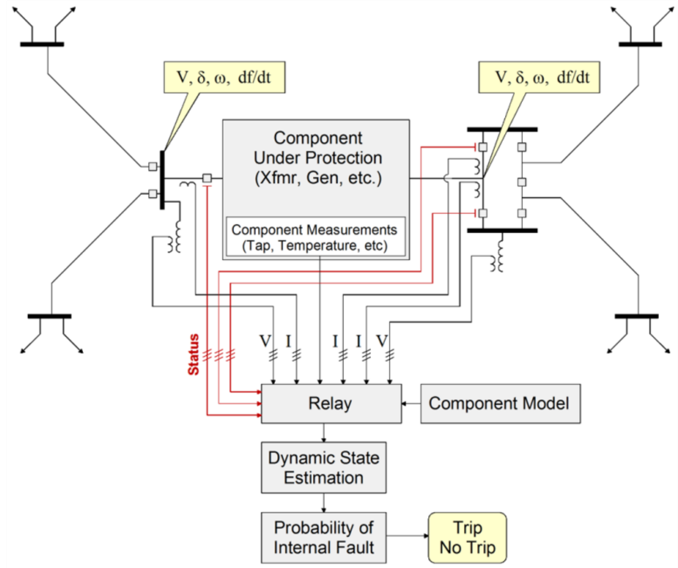

Figure 3. Illustration of Settingless Component Protection Scheme

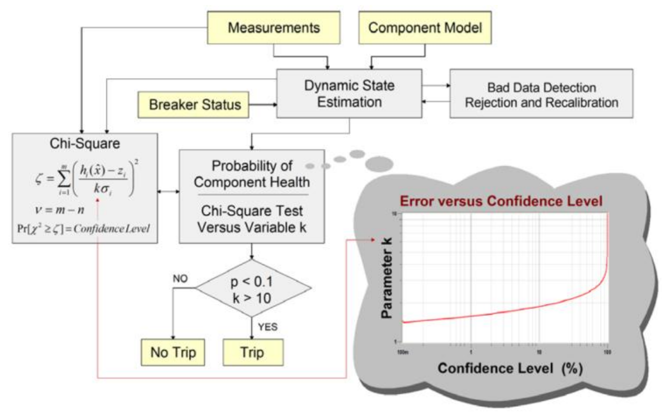

Figure 4. Illustration of Settingless Protection Logic

In general, the proposed method can identify any internal abnormality of the component within a cycle and trip the circuit breaker immediately. Furthermore, it does not degrade the security because a relay does not trip in the event of normal behavior of the component, for example inrush currents or over excitation currents in case of transformers, since in these cases the method produces a high confidence level that the normal behavior of the component is consistent with the model of the component. Note also that the method does not require any settings or any coordination with other relays.

III. Implementation of Setting-less Protection

The implementation of the setting-less protection is based on dynamic state estimation which can be a complex computational procedure. The complexity is reduced by using an object orientation approach that is enabled by a standard algebraic companion form (ACF) model. Specifically, any power system component can be express in the ACF standard form with the following standard syntax:

$$\begin{bmatrix} i(t) \\ 0 \\ i(t_m) \\ 0 \end{bmatrix} = Y_{eq}\begin{bmatrix} v(t) \\ y(t) \\ v(t_m) \\ y(t_m) \end{bmatrix} + \begin{bmatrix} \begin{bmatrix} v(t) \\ y(t) \\ v(t_m) \\ y(t_m) \end{bmatrix}^T \cdot F_{eq} \cdot \begin{bmatrix} v(t) \\ y(t) \\ v(t_m) \\ y(t_m) \end{bmatrix} \\ \vdots \end{bmatrix} - b_{eq} \quad (1)$$

where

$$b_{eq} = \sum_i A_i \cdot \begin{bmatrix} v(t-i\cdot h) \\ y(t-i\cdot h) \end{bmatrix} + \sum_i B_i \cdot \begin{bmatrix} i(t-i\cdot h) \\ 0 \end{bmatrix} + C,$$

t is the current time, h the time interval for one integration step, t_m the midpoint between t-h and t, $i(t)$ the current vector, $v(t)$ the voltage vector, $y(t)$ the internal state vector, Y_{eq}, A_i, and B_i coefficient matrices, F_{eq} the quadratization matrix, and C the constant vector. The derivation of the ACF from the dynamic device model is achieved with the following two steps: (1) model quadratization and (2) quadratic integration. The model quadratization reduces the model nonlinearities so that the dynamic model will consist of a set of linear and quadratic equations. The quadratic integration is a numerical integration method that is applied to the quadratic model assuming that the functions vary quadratically over the integration time step. This standardization allows the algorithmic handling of measurements and state estimation; in addition converts the dynamic state estimation into a state estimation that has the form of a static state estimation. The following subsections explain the two procedures (model quadratization and quadratic integration). Subsequently the utilization of the ACF for the dynamic state estimation is presented followed by the assessment of component health.

A. Model Quadratization

Model nonlinearities can be quadratized with the introduction of additional states and equations in such a way that the order is no greater than two [16], [17]. For example, the nonlinearity of the transformer saturable core can be characterized with the nonlinear function of the magnetizing current and the magnetic flux linkage as follows:

$$i_m(t) = i_0 \left| \frac{\lambda(t)}{\lambda_0} \right|^n sign(\lambda(t)) = 0, \quad (2)$$

where $i_m(t)$ is the magnetizing current, $\lambda(t)$ the magnetic flux linkage, i_0 and λ_0 equation constants, and *sign* the sign function. In this case, the number of additional internal states is determined by the following rule:

$$m = m_1 + m_2, \quad (3)$$

where m_1 = *int(log2(n))* and m_2 = *(# of ones in the binary representation of n) – 1*. Accordingly, the nonlinear function of the transformer can be quadratized as follows:

$$y_1(t) = (\lambda(t)/\lambda_0)^2, \quad (4)$$

$$y_2(t) = y_1(t)^2, \quad (5)$$

$$\vdots$$

$$y_{m_1}(t) = y_{m_1-1}(t)^2, \quad (6)$$

$$y_{m_1+1}(t) = y_{m_1}(t)\cdot y_{j1}(t), \quad (7)$$

$$y_{m_1+2}(t) = y_{m_1+1}(t)\cdot y_{j2}(t), \quad (8)$$

$$\vdots$$

$$\begin{cases} y_m(t) = y_{m-1}(t)\cdot y_{jm_2}(t), & if\ n\ even, \\ y_m(t) = y_{m-1}(t)\cdot \lambda(t)/\lambda_0, & if\ n\ odd, \end{cases} \quad (9)$$

$$i_m(t) = i_0 \cdot sign(\lambda(t))\cdot y_m(t), \quad (10)$$

where $j1$ to jm_2 are the internal state variables corresponding to the ones in the binary representation of n except the most significant bit. The advantage of model quadratization is that the model nonlinearity decreases to order two without altering the model. Of course this advantage is obtained at the price of increased dimensionality of the model.

B. Quadratic Integration Method

In an attempt to simplify the dynamic state estimation, the dynamic model of the component, which in general contains differential equations, is converted into an algebraic model by the quadratic integration method [14], [15]. This integration method, which is a special case of the class of methods known as collocation methods, is a fourth-order accurate method. Therefore, this method is more accurate than the traditional trapezoidal integration method and free from artificial numerical oscillations [15].

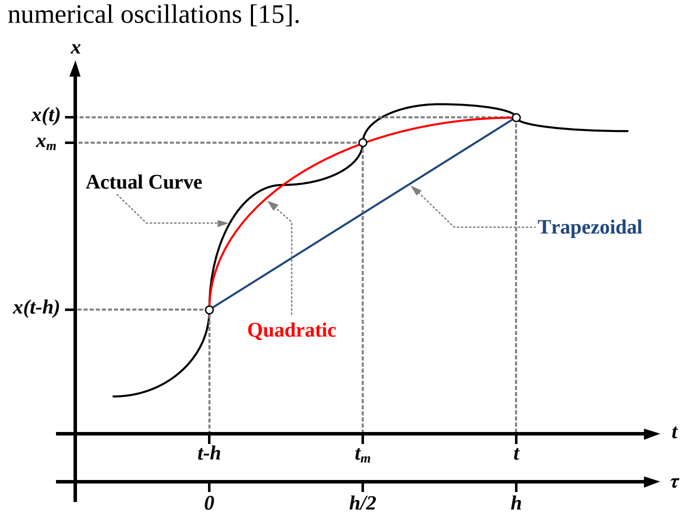

Figure 5. Quadratic Integration Method

The basic concept of quadratic integration method is that functions vary quadratically over the time period of one integration step, h as shown in Figure 5. The function $x(\tau)$ over one integration step [t-h to t] is a quadratic function expressed in terms of the values of the function at three points, as follows:

$$x(\tau) = a + b\tau + c\tau^2\,, \tag{11}$$

where

$$a = x(t-h)\,,$$

$$b = \frac{1}{h}\left(-3x(t-h) + 4x_m - x(t)\right),$$

$$c = \frac{2}{h^2}\left(x(t-h) - 2x_m + x(t)\right).$$

Subsequently each function in the quadratized model of the component is substituted with the expression in (2) and the result is integrated over the time step yielding the algebraic companion form of the component model. The procedure will be illustrated with a simple example. Consider the dynamic system represented with:

$$\frac{dx(t)}{dt} = Ax(t)\,, \tag{12}$$

where A is the coefficient matrix. If this equation is integrated, using the quadratic integration method, from t-h to t and from t-h to t-$h/2$, then the following matrix equation is obtained:

$$\begin{bmatrix} \frac{h}{24}A & I - \frac{h}{3}A \\ I - \frac{h}{6}A & \frac{2h}{3}A \end{bmatrix} \cdot \begin{bmatrix} x(t) \\ x_m \end{bmatrix} = \begin{bmatrix} I + \frac{5h}{24}A \\ I + \frac{h}{6}A \end{bmatrix} \cdot x(t-h)\,, \tag{13}$$

where I is the identity matrix. Note that (13) follows the standardized ACF, (1) exactly.

C. Object-Oriented Dynamic State Estimation

In the proposed dynamic state estimation, each measurement is an object that consists of the measured value and the corresponding function from the algebraic companion form of the component. Because the algebraic companion form is quadratic at most, the measurement model is also quadratic at most. Thus, the object-oriented measurement model can be expressed as the following standard equation:

$$\begin{aligned} z_k(t) &= \sum_i a_{i,t}^k \cdot x_i(t) + \sum_i a_{i,tm}^k \cdot x_i(t_m) \\ &+ \sum_{i,j} b_{i,j,t}^k \cdot x_i(t) \cdot x_j(t) \\ &+ \sum_{i,j} b_{i,j,tm}^k \cdot x_i(t_m) \cdot x_j(t_m) \\ &+ c_k(t) + \eta_k\,, \end{aligned} \tag{14}$$

where z is the measured value, t the current time, t_m the midpoint between the current and previous time, x the state variables, a the coefficients of linear terms, b the coefficients of nonlinear terms, c the constant term, and η the measurement error.

In general the measurements can be classified as across and through measurements. The across measurements have a simple model as fololws:

$$z_j(t) = x_j(t) + \eta_j\,. \tag{15}$$

The through measurement model is extracted from the algebraic companion form, i.e. the model is simply one equation of the AGC model, as follows:

$$z_j(t) = {Y_{eq}}^{(k)} \begin{bmatrix} v(t) \\ y(t) \\ v(t_m) \\ y(t_m) \end{bmatrix} + \begin{bmatrix} \begin{bmatrix} v(t) \\ y(t) \\ v(t_m) \\ y(t_m) \end{bmatrix}^T \cdot F_{eq} \cdot \begin{bmatrix} v(t) \\ y(t) \\ v(t_m) \\ y(t_m) \end{bmatrix} \\ \vdots \end{bmatrix}^{(k)} - {b_{eq}}^{(k)}\,, \tag{16}$$

where the superscript k means the kth row of the matrix or the vector.

In addition, the model can provide virtual measurements, in the form of equations that must be satisfied. Consider for example the ACF model equation below:

$$0 = {Y_{eq}}^{(k)} \begin{bmatrix} v(t) \\ y(t) \\ v(t_m) \\ y(t_m) \end{bmatrix} + \begin{bmatrix} \begin{bmatrix} v(t) \\ y(t) \\ v(t_m) \\ y(t_m) \end{bmatrix}^T \cdot F_{eq} \cdot \begin{bmatrix} v(t) \\ y(t) \\ v(t_m) \\ y(t_m) \end{bmatrix} \\ \vdots \end{bmatrix}^{(k)} - {b_{eq}}^{(k)}\,. \tag{17}$$

This equation is simply a relationship among the state os the component that must be satisfied. Therefore we can state that the zero value is a measurement that we know with certainty. We refer to this as a virtual measurement.

Eventually, all the measurement objects form the following measurement set:

$$z = h(x,t) + \eta\,, \tag{18}$$

where z is the measurement vector, x the state vector, h the vector of functions (at most quadratic), and η the vector of measurement errors.

The proposed dynamic state estimation is based on the weighted least squares (WLS). The objective function is formulated as follows:

$$Minimize\;\; J(x,t) = \left[z - h(x,t)\right]^T W \left[z - h(x,t)\right], \tag{19}$$

where W is the diagonal matrix whose non-zero entries are the inverse of the variance of the measurement errors. The solution can be finally obtained by the iterative method:

$$\hat{x}^{j+1} = \hat{x}^j + (H^T W H)^{-1} H^T W (z - h(\hat{x}^j, t))\,, \tag{20}$$

where $\hat{x}$ is the best estimate of states and H the Jacobian matrix of $h(x)$.

D. Component Health Index

The solution of the dynamic state estimation provides the best estimate of the dynamic state of the component. The well-known chi-square test provides the probability that the measurements are consistent with the dynamic state of the component. Thus the chi-square test quantifies the goodness of fit between the model and measurements (i.e., confidence level). The goodness of fit is expressed as the probability that the measurement errors are distributed within their expected range (chi-square distribution). The chi-square test requires two parameters: the degree of freedom (ν) and the chi-square critical value (ζ). In order to quantify the probability with one single variable, we introduce the variable k in the definition of the chi-square variable:

$$\nu = m - n, \qquad \zeta = \sum_{i=1}^{m} \left(\frac{h_i(\hat{x}) - z_i}{k\sigma_i} \right)^2 , \tag{21}$$

where m is the number of measurements, n the number of states, and $\hat{x}$ the best estimate of states. The goodness of fit (confidence level) can be finally obtained as follows:

$$\Pr[\chi^2 \geq \zeta(k)] = 1.0 - \Pr[\chi^2 \leq \zeta(k)] = 1.0 - \Pr(\zeta(k), \nu)\,. \tag{22}$$

The curve of confidence level versus chi-square critical value is depicted in Figure 6.

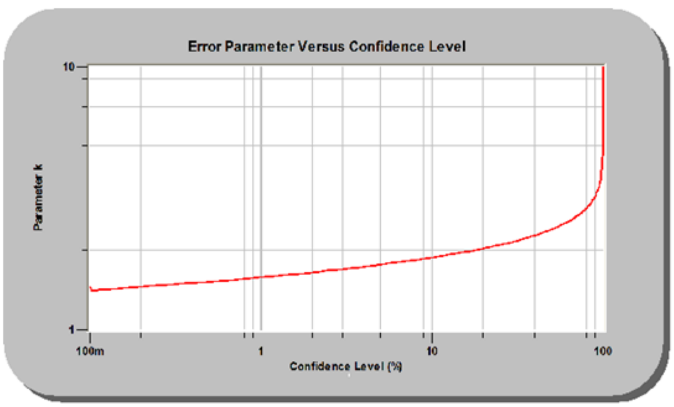

Figure 6. Confidence Level (%) vs Parameter k

The proposed method uses the confidence level as the health index of a component. A high confidence level indicates good fit between the measurement and the model, and thus we can conclude that the component has no internal fault. A low confidence level, however, implies inconsistency between the measurement and the model; therefore, we can conclude that an abnormality (internal fault) has occurred in the component.

It is important to point out that the component protection relay must not trip circuit breakers except when an internal fault occurs. For example, in case of a transformer, inrush currents or overexcitation currents, should be considered normal and the protection system should not trip the component. The proposed protection scheme can adaptively differentiate these phenomena from internal faults.

The proposed protection approach has been applied to several types of components (i.e. transformers, transmission lines, capacitor banks, etc.). We present an example of application of the proposed setting-less protection and its performance to a capacitor bank.

IV. Application to Capacitor Bank Protection

Shunt capacitor banks are used to improve the voltage profile, efficiency, and quality of the power system by providing capacitive compensation. The need for more sensitive and secure relaying schemes for capacitor banks, especially large banks at high voltage, has been increased, so we will discuss several critical applications essential for proper exemplification of the new capacitor bank protection scheme.

The operating conditions of capacitor banks during normal or transient state are 1) external faults, 2) inrush currents, and 3) internal faults (capacitor can failures, etc.). A single-line-to-ground-fault on or near busbar but outside the capacitor banks induces excessive outrush current that may trip overcurrent relays. Overcurrent relays should not trip for the outrush current. Moreover, any fault that occurred outside the capacitor banks should not operate the capacitor relays. It would be also necessary to prohibit relay operation for inrush current that may occur during switching operation of the capacitor banks. In contrast, unbalances that are induced by faulted elements or units of capacitor banks will damage the remaining intact capacitor elements or units and bring other undesirable consequences unless the capacitor bank is tripped promptly. In general, changes associated with capacitor element or unit failure become smaller as the rating of the capacitor bank increases and so the detection of these fault conditions becomes subtler. Therefore, it is necessary to detect and remove the internal fault of the capacitor banks using so sensitive protection schemes that can even detect a single internal element failure while avoiding nuisance tripping because of inrush current or outrush current.

The proposed protection scheme determines internal fault conditions with greater accuracy and certainty. Numerical experiments define the performance of the proposed protection scheme and its reliability. Sample numerical experiments are provided in the next section.

V. Numerical Experiments

The test system of the numerical experiments is shown in Figure 7. The system consists of a 15kV, 150MVA rated generator, an 18kV, 350MVA rated generator, a 15kV, 200MVA rated generator, transformers, transmission lines and a 115 kV capacitor bank in the substation model named CAP. The detailed model of the capacitor bank is shown in Figure 8. The numerical experiments are performed as follows. First a specific event is simulated, for example an external fault, a capacitor unit failure, etc., and the results are stored in a COMTRADE file. Subsequently, the proposed setting-less protection relay reads the data from the COMTRADE file, one set of measurements at a time and performs the setting-less protection algorithm. The results of the algorithm, such as estimated dynamic state of the capacitor bank, confidence level, etc. are also stored in a COMTRADE file for further view and analysis. The results for several events are presented next.

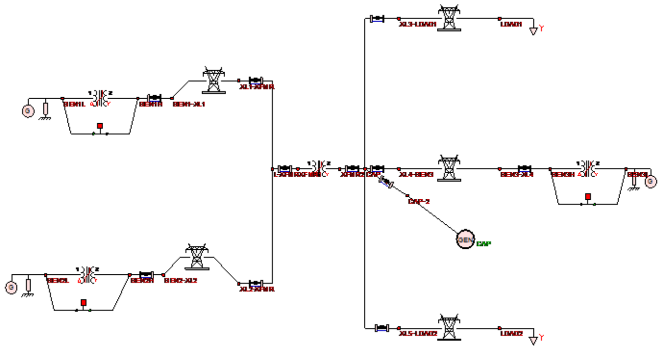

Figure 7. Test System for Numerical Experiments

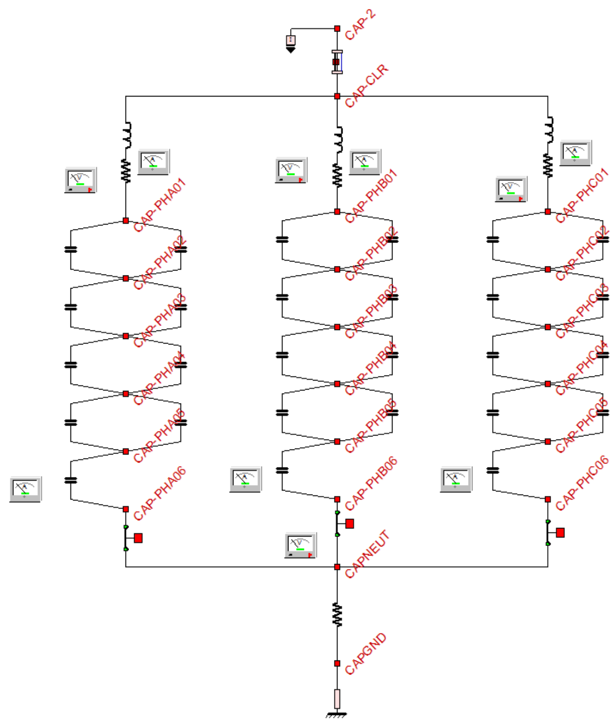

Figure 8. Detailed Capacitor Bank Model - Wye-Connected

1) External Fault

A single line to ground fault has been simulated on the right side of the transformer in the middle of the test system of Figure 7. This is an external fault for the capacitor bank but very close to the capacitor bank. The fault is cleared in 0.05 seconds after fault initiation. Figure 9 illustrates the simulation results during the fault and before and after the fault.

Figure 10 depicts some of the results of the settingless protection relay, specifically the estimated voltages at the three phases and the neutral (red) shown together with the measured voltages (blue), and the confidence level. As indicated in Figure 10 the health of monitored capacitor bank is high with 100% confidence level during the normal operation condition. During the external fault condition, transient voltage and current values resulting in 0% confidence level are measured for a short period of time (half cycle). For the remaining period of the fault conditions, the index is 100% indicating that the fault is external to the capacitor bank. The relay will not trip.

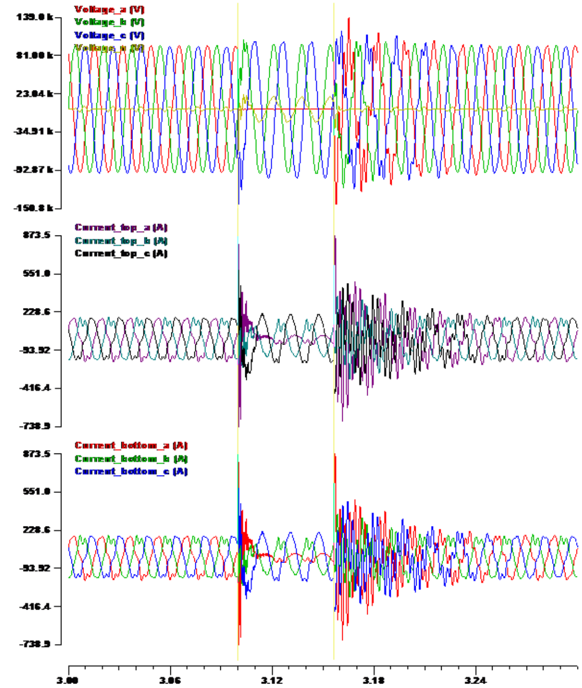

Figure 9. Simulation Results for an External Fault Event: Measured Signals at the Capacitor Bank

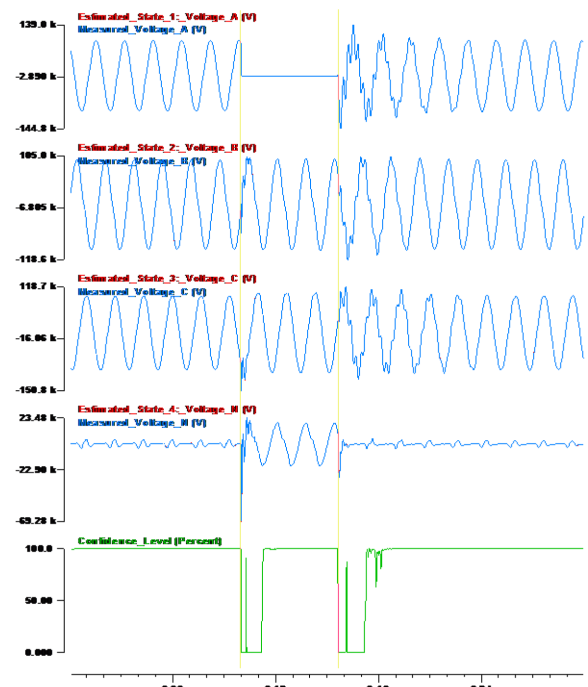

Figure 10. External Fault Event: Measured and Estimated Values, Confidence Level

2) *Internal Fault*

A single unit failure has been simulated for the capacitor bank of the test system of Figure 7. This is an internal fault for the capacitor bank. The fault is cleared in 0.065 seconds after fault initiation. Figure 11 illustrates the simulation results during the fault and before and after the fault. Note that the disturbance does not appear to be substantial as it is usually the case.

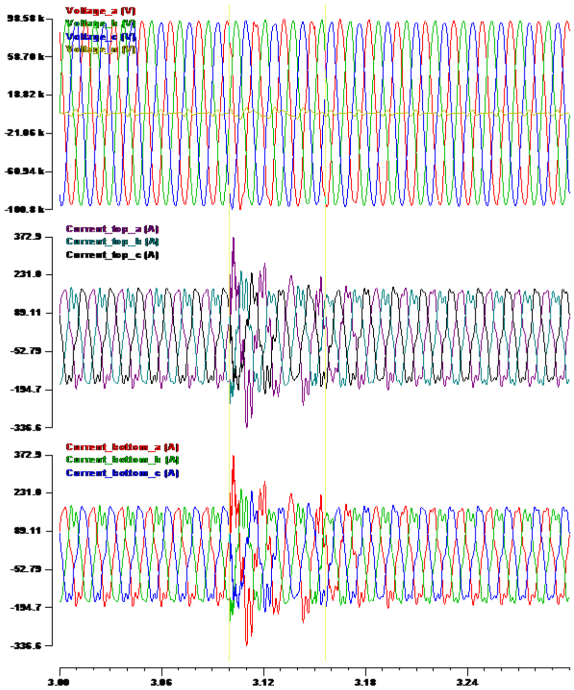

Figure 11. Simulation Results for an Internal Fault Event: Measured Signals at the Capacitor Bank

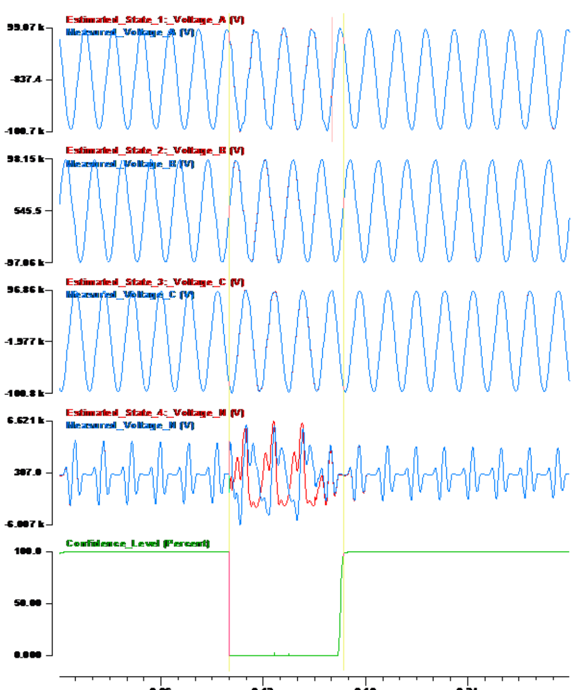

Figure 12. Internal Fault Event: Measured and Estimated Values, Confidence Level

Figure 12 depicts some of the results of the settingless protection relay, specifically the estimated voltages at the three phases and the neutral (red) shown together with the measured voltages (blue), and the confidence level. As indicated in Figure 12 the health of monitored capacitor bank is zero confidence level during the internal fault. The relay will trip on this event. Note that the relay is able to determine the internal fault even if the disturbance is very small.

VI. Further Work

The proposed setting-less protection method based on dynamic state estimation promises to be an effective, reliable and secure protection scheme. We plan to evaluate the performance of the proposed method via numerical experiments on a number of components, i.e. transmission lines, transformers, generators, motors, etc. and address issues such as the impact of instrumentation channel characteristics, GOPS synchronized measurements, required communications in case that component terminals are far apart, etc. Once numerical experiments are completed, the plan is to perform field trials in parallel with conventional protection schemes.

VII. Conclusion

In this paper, we proposed a new protection scheme that can adaptively diagnose the health condition of the component under protection. The approach leads to protection schemes that do not require settings or the settings are simplified. The proposed method can differentiate internally faulted components from unfaulted conditions; for example, in case of transformer protection, the method can identify the high inrush current and/or over excitation currents as normal operation, while it can identify a fault near the neutral of the transformer.

The proposed method is based on dynamic state estimation using real-time measurement data and the dynamic model of the component; the real-time measurement data are continuously provided by online monitoring system. From these measurements and the dynamic model, the dynamic state estimation produces the real-time dynamic states of the component as well as the confidence level that indicates the goodness of fit of the component model to the measurements. This confidence level is used to assess the health of the component; if the confidence level is almost zero, then we can conclude that any internal fault has occurred inside the component.

This paper demonstrated the proposed protection scheme with numerical experiments on a 115 kV capacitor bank.

Finally, the setting-less protection method presented in this paper can be applied to other components in power system such as generators, lines, cables, motors, etc.

VIII. Acknowledgments

The work in this paper was partially supported by the DoE/NETL project DE-OE0000117 and EPRI (Power System Engineering Research Center project S48). Their support of this work is gratefully acknowledged.

IX. References

[1] J. H. Harlow, *Electric power transformer engineering*, 2nd ed.: CRC Press, 2007.

[2] S. Patel, "Fundamentals of transformer inrush," in *Proc. the 65th Annual Georgia Tech Protective Relaying Conference*, May 2011.

[3] R. Hunt, J. Schaefer, and B. Bentert, "Practical experience in setting transformer differential inrush restraint," in *Proc. the 61st Annual Conference for Protective Relay Engineers*, Apr. 2008, pp. 118-141.

[4] *IEEE Guide for the Protection of Shunt Capacitor Banks*, IEEE Std C37.99-2000 (Revision of IEEE Std C37.99-1990), Jan. 2000.

[5] G. Gopakumar, H. Yan, B. A. Mork, and K. K. Mustaphi, "Shunt capacitor bank switching transients: A tutorial and case study," in *Proc. Minnesota Power Systems Conference*, 1999.

[6] S. K. Buggaveeti and S. M. Brahma, "Improved overcurrent protection of capacitor banks using mathematical morphology," *IEEE Trans. Power Delivery,* vol. 26, no. 3, pp. 1972-1979, Jul. 2011.

[7] F. J. Nepveux, "Protection of tuned capacitor banks," *IEEE Trans. Industry Applications,* vol. 44, no. 4, pp. 973-978, Jul. 2008.

[8] L. Wei-Jen, K. Narayanan, T. Maffetone, and P. Didsayabutra, "The design of a capacitor bank early warning system," *IEEE Trans. Industry Applications,* vol. 39, no. 2, pp. 306-312, Mar. 2003.

[9] B. Kasztenny, J. Schaefer, and E. Clark, "Fundamentals of adaptive protection of large capacitor banks - accurate methods for canceling inherent bank unbalances," in *Proc. 60th Annual Conference for Protective Relay Engineers*, Mar. 2007, pp. 126-157.

[10] E. Farantatos, G. K. Stefopoulos, G. J. Cokkinides, and A. P. S. Meliopoulos, "PMU-based dynamic state estimation for electric power systems," in *Proc. IEEE PES General Meeting*, Jul. 2009.

[11] R. Huang, E. Farantatos, G. J. Cokkinides, and A. P. S. Meliopoulos, "Substation based dynamic state estimator - numerical experiment," in *Proc. IEEE PES Transmission and Distribution Conference and Exposition*, New Orleans, Apr. 2010.

[12] A. P. S. Meliopoulos, G. J. Cokkinides, F. Galvan, B. Fardeanesh, and P. Myrda, "Delivering accurate and timely data to all," *IEEE Power and Energy Magazine,* vol. 5, no. 3, pp. 74-86, May 2007.

[13] A. P. S. Meliopoulos, G. J. Cokkinides, C. Hedrington, and T. L. Conrad, "The supercalibrator - a fully distributed state estimator," in *Proc. IEEE PES General Meeting*, Jul. 2010.

[14] A. P. Meliopoulos, G. J. Cokkinides, and G. K. Stefopoulos, "Improved numerical integration method for power/power electronic systems based on three-point collocation," in *Proc. the 44th IEEE Conference on Decision and Control, and European Control Conference*, Dec. 2005, pp. 6780-6787.

[15] A. P. S. Meliopoulos, G. J. Cokkinides, and G. Stefopoulos, "Quadratic integration method," in *Proc. International Power System Transients Conference*, Montreal, Jun. 2005.

[16] G. Stefopoulos, G. J. Cokkinides, and A. P. S. Meliopoulos, "Expert symbolic transient simulator based on quadratic integration method," in *Proc. the 13th International Conference on Intelligent Systems Application to Power Systems*, Nov. 2005, pp. 347-353.

[17] G. K. Stefopoulos, G. J. Cokkinides, and A. P. S. Meliopoulos, "Quadratized model of nonlinear saturable-core inductor for time-domain simulation," in *Proc. IEEE PES General Meeting*, Jul. 2009.

[18] *Integrated grounding system for windows (WinIGS)*, Advanced Grounding Concepts, Atlanta, GA. [Online]. Available: http://www.ap-concepts.com

[19] *IEEE Standard Common Format for Transient Data Exchange (COMTRADE) for Power Systems*, IEEE Std C37.111-1999, Mar. 1999.

X. Biographies

A. P. Sakis Meliopoulos (M '76, SM '83, F '93) was born in Katerini, Greece, in 1949. He received the M.E. and E.E. diploma from the National Technical University of Athens, Greece, in 1972; the M.S.E.E. and Ph.D. degrees from the Georgia Institute of Technology in 1974 and 1976, respectively. In 1971, he worked for Western Electric in Atlanta, Georgia. In 1976, he joined the Faculty of Electrical Engineering, Georgia Institute of Technology, where he is presently a professor. He is active in teaching and research in the general areas of modeling, analysis, and control of power systems. He has made significant contributions to power system grounding, harmonics, and reliability assessment of power systems. He is the author of the books, Power Systems Grounding and Transients, Marcel Dekker, June 1988, Ligthning and Overvoltage Protection, Section 27, Standard Handbook for Electrical Engineers, McGraw Hill, 1993, and the monograph, Numerical Solution Methods of Algebraic Equations, EPRI monograph series. Dr. Meliopoulos is a member of the Hellenic Society of Professional Engineering and the Sigma Xi.

George Cokkinides (M '85) was born in Athens, Greece, in 1955. He obtained the B.S., M.S., and Ph.D. degrees at the Georgia Institute of Technology in 1978, 1980, and 1985, respectively. From 1983 to 1985, he was a research engineer at the Georgia Tech Research Institute. Since 1985, he has been with the University of South Carolina where he is presently an Associate Professor of Electrical Engineering. His research interests include power system modeling and simulation, power electronics applications, power system harmonics, and measurement instrumentation. Dr. Cokkinides is a member of the IEEE/PES.

Sungyun Choi (S '09) received a B.E. degree in electrical engineering from Korea University in Seoul, Korea, in 2002 and an M.S. degree from the Georgia Institute of Technology in Atlanta, in 2009. He is currently pursuing a Ph.D. degree, working in the Power System Control and Automation Laboratory at the Georgia Institute of Technology. He worked as a network and systems engineer in Korea. His research interest lies in distributed power system automation and control, power system protection, communication networks, and systems in substation automation.

Yonghee Lee (S '10) was born in Seoul, Korea, in 1982. He obtained his B.S.E.E from Yonsei University, Korea in 2007. He started his graduate studies in Georgia Institute of Technology from 2008 fall semester. He is now pursuing MS / Ph. D degree under the advisory of Prof A. P. Meliopoulos. His research interests include PMU Device Testing, System Estimation (Static, Dynamic), Power System Control Using Smart Grid Concept, and Distribution Line Protection.